

Novel Bimetallic Thiocarboxylate Compounds as Single-Source Precursors to Binary and Ternary Metal Sulfide Materials

Theivanayagam C. Deivaraj,[†] Jin-Ho Park,[‡] Mohammad Afzaal,[‡]
Paul O'Brien,^{*,‡} and Jagadese J. Vittal^{*,†}

Department of Chemistry, National University of Singapore, Singapore 117543, and
The Manchester Materials Science Centre and Department of Chemistry,
The University of Manchester, Oxford Road, Manchester, UK M13 9PL

Received January 28, 2003. Revised Manuscript Received March 24, 2003

The binuclear compounds [(Ph₃P)CuM(SC{O}Ph)₄] (M = Ga (**1**) or In (**2**)), [(Ph₃P)₂AgGa(SC{O}Ph)₄] (**3**), [(Ph₃P)₂AgIn(SC{O}R)₄] (R = Me (**4**) or Ph (**5**)) have been synthesized and characterized. The solid-state structures of compounds **1–3** have been determined by X-ray crystallography. Thermogravimetry and pyrolysis studies revealed that these compounds decompose to give the corresponding ternary metal sulfide materials. However, using the aerosol-assisted chemical vapor deposition (AACVD) method, In₂S₃ thin films were obtained from **2** and AgIn₅S₈ thin films were obtained from compounds **4** and **5**.

Introduction

Metal sulfides find a wide variety of applications, e.g., in photovoltaics and optoelectronic devices, and hence there has been considerable interest in synthesizing single-source precursors for these materials.^{1–4} Such precursors have been considered as attractive sources for bulk materials, thin films, or nanoparticles. Among such materials, CuInS₂ with a band gap of 1.53 eV at ambient temperature is considered a good candidate for photovoltaic applications.⁵ Solar cells fabricated with thin films of CuInS₂ have light-conversion efficiencies of ca. 7%.⁶ CuGaS₂ has a wide band gap (2.49 eV) and is used in green light emitting diodes.⁷ AgInS₂, AgIn₅S₈, and AgGaS₂ are used as linear and nonlinear optical materials.^{8,9} Despite these many potential applications for ternary materials such as MM'S₂ (M = Cu or Ag and M' = Ga or In), single-source precursors for these materials are rare. Kanatzidis et al. have prepared and characterized compounds of the general formula (Ph₃P)₂-Cu(μ-ER)₂In(ER)₂ (E = S or Se and R = Et or *iso*-Bu). The single-crystal structures of these compounds have also been reported.¹⁰ These compounds, when subjected

to pyrolysis, yielded the corresponding ternary materials. Buhro and co-workers have used (Ph₃P)₂Cu(μ-SEt)₂In(SEt)₂ to obtain thin films of CuInS₂ using spray MOCVD.¹¹ Nomura et al. have prepared a compound of the formula [Bu₂In(SPr)Cu(S₂CNPr₂)] and used it to deposit thin films of CuInS₂.¹² These authors have also reported the deposition of CuInS₂ by solution pyrolysis of Bu₂InSPr and Cu(S₂CNBu₂)₂.¹³ Recently, two liquid compounds, [(*n*-Bu₃P)₂Cu(SR)₂In(SR)₂] (R = Et and *n*-Pr) have been successfully used to deposit CuInS₂ thin films.^{14,15} As a part of our ongoing explorations of metal–thiocarboxylate systems,^{16–27} we have now devoted attention to the syntheses of single-source molec-

* For correspondence: paul.obrien@man.ac.uk (P.O.B.) or chmjiv@nus.edu.sg (J.J.V.).

[†] National University of Singapore.

[‡] The University of Manchester.

- (1) Bochmann, M. *Chem. Vap. Deposition* **1996**, *2*, 85.
- (2) O'Brien, P.; Nomura, R. *J. Mater. Chem.* **1995**, *5*, 1761.
- (3) Lazell, M.; O'Brien, P.; Otway, D. J.; Park, J. H. *J. Chem. Soc., Dalton Trans.* **2000**, 4479.
- (4) Gleizes, A. N. *Chem. Vap. Deposition* **2000**, *6*, 155.
- (5) Thiel, F. A. *J. Electrochem. Soc.* **1982**, *129*, 1570.
- (6) Wu, Y. L.; Lin, H. Y.; Sun, C. Y.; Yank, M. H.; Hwang, H. L. *Thin Solid Films* **1989**, *168*, 113.
- (7) Oishi, K.; Kobayashi, S.; Ohta, S. I.; Tsuboi, N.; Kaneko, F. *J. Cryst. Growth* **1997**, *177*, 88.
- (8) Abrahams, S. C.; Bernstein, J. L. *J. Chem. Phys.* **1973**, *59*, 1625.
- (9) Yonenga I.; Sumino, K.; Niwa, E.; Masumoto, K. *J. Cryst. Growth* **1996**, *167*, 616.
- (10) Hirpo, W.; Dhingra, S.; Sutorik, A. C.; Kanatzidis, M. G. *J. Am. Chem. Soc.* **1993**, *115*, 1597.

- (11) Hollingsworth, J. A.; Hepp, A. F.; Buhro, W. E. *Chem. Vap. Deposition* **1999**, *5*, 105.
- (12) Nomura, R.; Seki, Y.; Matsuda, H. *J. Mater. Chem.* **1992**, *2*, 765.
- (13) Nomura, R.; Fujii, S.; Kanaya, K.; Matsuda, H. *Polyhedron* **1990**, *9*, 361.
- (14) Banger, K. K.; Harris, J. D.; Cowen, J. E.; Hepp, A. F. *Thin Solid Films* **2002**, *403–404*, 390.
- (15) Banger, K. K.; Cowen, J.; Hepp, A. F. *Chem. Mater.* **2001**, *13*, 3827.
- (16) Vittal, J. J.; Dean, P. A. W. *Inorg. Chem.* **1993**, *32*, 791.
- (17) Vittal, J. J.; Dean, P. A. W. *Inorg. Chem.* **1996**, *35*, 3089.
- (18) Vittal, J. J.; Dean, P. A. W.; Craig, D. C.; Scudder, M. L. *Inorg. Chem.* **1998**, *37*, 1661.
- (19) Devy, R.; Vittal, J. J.; Dean, P. A. W. *Inorg. Chem.* **1998**, *37*, 6939.
- (20) Sampanthar, J. T.; Deivaraj, T. C.; Vittal, J. J.; Dean, P. A. W. *J. Chem. Soc., Dalton Trans.* **1999**, 4419.
- (21) Sampanthar, J. T.; Vittal, J. J.; Dean, P. A. W. *J. Chem. Soc., Dalton Trans.* **1999**, 3153.
- (22) Deivaraj, T. C.; Lai, G. X.; Vittal, J. J. *Inorg. Chem.* **2000**, *39*, 1028.
- (23) Deivaraj, T. C.; Dean, P. A. W.; Vittal, J. J. *Inorg. Chem.* **2000**, *39*, 3071.
- (24) Deivaraj, T. C.; Vittal, J. J. *J. Chem. Soc., Dalton Trans.* **2001**, 322.
- (25) Deivaraj, T. C.; Vittal, J. J. *J. Chem. Soc., Dalton Trans.* **2001**, 329.
- (26) Deivaraj, T. C.; Lye, W. H.; Vittal, J. J. *Inorg. Chem.* **2002**, *41*, 3755.
- (27) Lin, M.; Loh, K. P.; Deivaraj, T. C.; Vittal, J. J. *Chem. Commun.* **2002**, 1400.

ular precursors for I–III–VI materials. A preliminary account of this study has been published earlier.²⁸ In this paper we report on the synthesis and characterization of compounds of the type [(Ph₃P)CuM(SC{O}Ph)₄] (M = Ga (**1**) or In (**2**)), [(Ph₃P)₂AgGa(SC{O}Ph)₄] (**3**), and [(Ph₃P)₂AgIn(SC{O}R)₄] (R = Me (**4**) or Ph(**5**)), their thermal properties, and results of AACVD experiments.

Experimental Section

General. All materials were obtained commercially and used as received. The solvents were dried by allowing them to stand over 3-Å molecular sieves overnight. The preparations were carried out under nitrogen atmosphere and the yields are reported with respect to the metal salts. The compounds are fairly stable but were stored under nitrogen at 5 °C to avoid any decomposition. The starting material Ga(NO₃)₃·xH₂O (x ≈ 3 by TG analysis) was purchased from Aldrich and [(Ph₃P)₂Cu(NO₃)] was prepared by a literature method.²⁹ Compounds **4** and **5** were prepared as described earlier.²⁸

Synthesis of [(PPh₃)Cu(μ-SC{O}Ph-S)(μ-SC{O}Ph-S,O)₂-Ga(SC{O}Ph)] (1**).** To NaSC{O}Ph formed in situ (by reacting PhC{O}SH (184 μL, 1.56 mmol) and Na (0.04 g, 1.56 mmol) in MeOH (15 mL)), 0.1 g of Ga(NO₃)₃·3H₂O (0.32 mmol) in MeOH (10 mL) was added to get a yellow solution and was followed by the addition of (Ph₃P)₂Cu(NO₃) (0.25 g, 0.39 mmol) in CH₂Cl₂ (15 mL). The orange solution thus obtained was stirred and the solvents were removed under a flow of N₂. The product obtained as red oil along with some yellow powder was extracted with CH₂Cl₂ (20 mL), and the resulting red solution was separated and layered with petroleum ether. Reddish yellow crystals were obtained the following day. The crystals of **1** were collected, washed with petroleum ether, and dried under vacuum. Yield 0.27 g (89%); mp 163 °C (decomposition). Anal. Calcd for C₄₆H₃₅O₄S₄PCuGa (mol wt 944.29): C, 58.51; H, 3.74. Found: C, 58.48; H, 3.77. ¹³C NMR (CDCl₃) δ, ppm thiobenzoate ligand: 127.3 (C_{2/6} or C_{3/5}), 128.3 (C_{2/6} or C_{3/5}), 131.4 (C₄), 138.8 (C₁), 202.9 (PhCOS). PPh₃: 128.6 (C₃, ³J(P–C) = 8.7 Hz), 129.6 (C₄), 132.9 (C₁, ¹J(P–C) = 27.2 Hz), 133.7 (C₂, ²J(P–C) = 15.2 Hz). ³¹P NMR: δ, ppm –1.54 (s). Selected IR data: 1594.9 (w, C=O) and 983.7 (s, C–S) cm⁻¹.

Synthesis of [(PPh₃)Cu(μ-SC{O}Ph-S,O)₂(μ₂-SC{O}Ph-S₂,O)In(SC{O}Ph)] (2**).** The compound was synthesized using a procedure similar to **1** but Ga(NO₃)₃·3H₂O was replaced by InCl₃·4H₂O. Yield 69%; mp 185 °C (melting with decomposition). Anal. Calcd for C₄₆H₃₅O₄S₄PCuIn·0.5 CH₂Cl₂ (mol wt 1031.85): C, 54.13; H, 3.52. Found: C, 54.38; H, 3.74. ¹³C NMR (CDCl₃) δ, ppm thiobenzoate ligand: 127.9 (C_{2/6} or C_{3/5}), 129.3 (C_{2/6} or C_{3/5}), 133.1 (C₄), 137.7 (C₁), 206.7 (PhCOS). PPh₃: 128.5 (C₃, ³J(P–C) = 8.7 Hz), 129.6 (C₄), 132.8 (C₁, ¹J(P–C) = 20.0 Hz), 133.7 (C₂, ²J(P–C) = 14.2 Hz). ³¹P NMR: δ, ppm –1.57. Selected IR data: 1594.5 (s, C=O), 950.0 (s, C–S) cm⁻¹.

[(PPh₃)₂Ag(μ-SC{O}Ph-S)Ga(SC{O}Ph)₃] (3**).** A solution of PPh₃ (0.21 g, 0.78 mmol) in 15 mL of MeCN was added to a solution of AgNO₃ (0.07 g, 0.39 mmol) in 10 mL of MeCN and stirred for about 10 min to obtain a precipitate of (PPh₃)₂AgNO₃. The solvents were evaporated, and the resulting white solid, dissolved in 20 mL of CHCl₃, was added to Ga(NO₃)₃·3H₂O (0.1 g, 0.39 mmol) in 12 mL of MeOH. To this solution, C₆H₅COSNa (prepared in situ by reacting C₆H₅COSH (184 μL, 1.56 mmol) with Na (0.036 g, 1.564 mmol) in 15 mL of MeOH) was added. The resulting bright yellow solution was stirred for 30 min and then the solvents were removed by a flow of N₂. The product was extracted with CHCl₃ (15 mL) and filtered immediately, and the filtered product was layered with petroleum ether and stored at 5 °C. Colorless crystals of **3** thus

obtained were filtered, washed with Et₂O, and dried under vacuum. Yield 0.37 g (76%); mp 167 °C (melting with decomposition). Anal. Calcd for C₆₄H₅₀O₄S₄P₂AgGa (mol wt 1250.9): C, 61.45; H, 4.02. Found: C, 61.87; H, 4.06. ¹³C NMR (CDCl₃) δ, ppm thiobenzoic acid ligand: 127.7 (C_{2/6} or C_{3/5}), 128.3 (C_{2/6} or C_{3/5}), 131.6 (C₄), 140.6 (C₁), 201.0 (PhCOS). PPh₃: 128.6 (C₃, ³J(P–C) = 9.8 Hz), 129.7 (C₄), 133.0 (C₁, ¹J(P–C) = 20.7 Hz), 133.8 (C₂, ²J(P–C) = 16.3 Hz). ³¹P NMR: δ, ppm 6.53. IR data (cm⁻¹): 1569.4 (s, C=O), 973.8 (w, C–S).

Instruments and Characterization. The ¹³C{¹H} and ³¹P{¹H} NMR spectra were recorded on a Bruker ACF300 FTNMR spectrometer using TMS as internal and 85% H₃PO₄ as external reference at 25 °C. The IR spectra (KBr pellet) were recorded using a Bio-Rad FTIR spectrometer. The elemental analyses were performed by the microanalytical laboratory of the chemistry department, National University of Singapore. Thermogravimetric analyses were carried out using a SDT 2980 TGA thermal analyzer with a heating rate of 10 °C min⁻¹ in N₂ atmosphere using a sample size of 5–10 mg per run. X-ray powder patterns were obtained using a D5005 Bruker AXS X-ray diffractometer. Pyrolysis experiments were carried out in a horizontal tube furnace in a quartz reaction chamber. The quartz reactor was subjected to dynamic vacuum of about 0.5 Torr. The SEM images were obtained from a JEOL JSM-T220A instrument for bulk materials and a Philips XL30 FEG for thin films and EDAX analyses. The XPS measurements were performed in the ultrahigh vacuum chamber (base pressure of 10⁻⁸ Pa) of an ESCA 300 spectrometer using Mg Kα excitation. The energy scale was calibrated using Au and argon ions were used for etching.

X-ray Crystallography. The diffraction experiments were carried out at 20 °C on a Bruker SMART CCD diffractometer with Mo Kα radiation from a sealed tube. The program SMART³⁰ was used for collecting frames of data, indexing reflections, and determination of lattice parameters; SAINT³⁰ was used for integration of the intensity of reflections and scaling. SADABS³¹ was used for absorption correction, and SHELXTL³² was used for space group and structure determination and least-squares refinements on *I*². The relevant crystallographic data and refinement details are shown in Table 1. The phenyl ring of the thiobenzoate anion (C31–C36) in **1** was found to be disordered. Two disorder models with equal occupancies were refined for the same. There are 3.5 CHCl₃ solvent molecules present in **3**. All the solvent molecules were disordered and were treated with a soft SADI restraint on C–Cl and Cl···Cl distances. Disorder models were resolved for the CHCl₃ molecules. One molecule is disordered over two positions with occupancies of 0.55 and 0.45. Another CHCl₃ molecule is disordered over three locations with occupancies of 0.6, 0.25, and 0.15. The half molecule of CHCl₃ present in **3** is also disordered over two locations with occupancies of 0.3 and 0.2.

Aerosol-Assisted Chemical Vapor Deposition (AACVD). Approximately 0.25 g of precursor was dissolved in 30 mL of toluene (or THF) in a round-bottomed flask. Six glass substrates (1 × 2 cm) were placed inside the reactor tube. The carrier gas flow rate was controlled by Platon flow gauges. The solution in the flask was placed in a water bath above the piezoelectric modulator of a humidifier in which aerosol droplets were generated and transferred by the carrier gas (N₂, flow rate 180 sccm) into the hot-wall zone. Then both the solvent and the precursor were evaporated, and the precursor vapor reached the heated substrate surface where thermally induced reactions and film deposition took place. This home-made aerosol-assisted chemical vapor deposition kit consisted of a two-necked flask, a PIFCO ultrasonic humidifier (model 1077) and a Carbolite furnace.

(30) SMART & SAINT Software Reference Manuals, Version 4.0; Siemens Energy & Automation, Inc.: Analytical Instrumentation; Madison, WI, 1996.

(31) Sheldrick, G. M. SADABS Software for Empirical Absorption Correction; University of Göttingen: Göttingen, Germany, 2000.

(32) SHELXTL Reference Manual, Version 5.1; Bruker Analytical X-ray Systems, Inc.: Madison, WI, 1997.

(28) Deivaraj, T. C.; Park, J.-H.; Afzaal, M.; O'Brien, P.; Vittal, J. J. Chem. Commun. 2001, 2304.

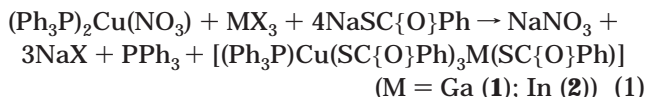
(29) Kubas, G. J. Inorg. Synth. 1970, 19, 93.

Table 1. Crystal Data and Structure Refinement for 1–3

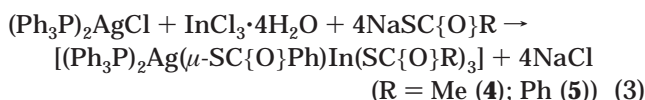
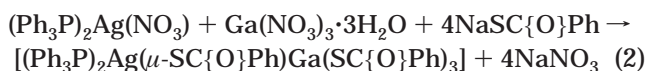
	1	2	3
chemical formula	C ₄₆ H ₃₅ CuGaO ₄ PS ₄	C ₄₆ H ₃₅ CuInO ₄ PS ₄ ·0.5 CH ₂ Cl ₂	C ₆₄ H ₅₀ O ₄ S ₄ P ₂ AgGa·3.5 CHCl ₃
formula weight	944.21	1031.77	1668.60
temperature, °C	20	20	–50
λ, Å	0.71073	0.71073 Å	0.71073
crystal system	monoclinic	triclinic	triclinic
space group	P2 ₁ /c	P1	P1
unit cell dimensions			
<i>a</i> , Å	13.0239(2)	10.5914(1)	15.0668(7)
<i>b</i> , Å	9.2656(2)	11.8903(1)	15.3124(7)
<i>c</i> , Å	36.1156(8)	19.6156(3)	18.6217(8)
α, deg	90	74.151(1)	101.240(1)
β, deg	94.320(1)	77.889(1)	113.171(1)
γ, deg	90	77.254(1)	95.551(1)
<i>V</i> , Å ³	4345.8(2)	2288.19(5)	3801.6(3)
<i>Z</i>	4	2	2
ρ, g/cm ³	1.443	1.498	1.458
μ, mm ^{–1}	1.381	1.286	1.177
<i>F</i> (000)	1928	1042	1682
θ range, deg	1.86 to 26.37	1.81 to 26.37	2.04 to 25.00
index ranges	–16 ≤ <i>h</i> ≤ 16 –11 ≤ <i>k</i> ≤ 11 –30 ≤ <i>l</i> ≤ 45	–13 ≤ <i>h</i> ≤ 12 –14 ≤ <i>k</i> ≤ 13 –24 ≤ <i>l</i> ≤ 16	–17 ≤ <i>h</i> ≤ 17 –18 ≤ <i>k</i> ≤ 15 –17 ≤ <i>l</i> ≤ 22
reflections collected	22503	13171	22382
independent reflections	8684, <i>R</i> _{int} = 0.0670	8996, <i>R</i> _{int} = 0.0272	13374, <i>R</i> _{int} = 0.0219
data/restraints/parameters	8684/0/474	8996/1/542	13374/84/803
GOF on <i>F</i> ²	1.094	1.054	1.028
final <i>R</i> indices (<i>I</i> > 2σ(<i>I</i>))	<i>R</i> 1 = 0.0858 w <i>R</i> 2 = 0.1903	<i>R</i> 1 = 0.0398 w <i>R</i> 2 = 0.1105	<i>R</i> 1 = 0.0670 w <i>R</i> 2 = 0.1989
<i>R</i> indices (all data)	<i>R</i> 1 = 0.1327 w <i>R</i> 2 = 0.2161	<i>R</i> 1 = 0.0531 w <i>R</i> 2 = 0.1162	<i>R</i> 1 = 0.0852 w <i>R</i> 2 = 0.2124
extinction coefficient		0.0010(3)	
largest difference peak and hole, e·Å ^{–3}	1.180 and –0.783	1.081 and –0.656	2.003 and –1.320

Results and Discussion

Synthesis. The compounds [(Ph₃P)Cu(μ-SC{O}Ph)₃M(SC{O}Ph)] (M = Ga(1) or In(2)) were prepared by reacting bis-triphenylphosphinecopper(I) nitrate with the appropriate [M(SC{O}Ph)₄][–] anion as shown below in eq 1. In the resulting bimetallic complexes the copper atoms are bonded to the sulfur centers of the thiobenzoate ligands and only to one PPh₃ unit.



Attempts to isolate the thioacetate analogues of 1 and 2 using a similar synthetic method were unsuccessful. Compounds 1 and 2 were fairly stable, however, they were stored at 5 °C in sample vials purged with nitrogen. From reactions of (Ph₃P)₂Ag(NO₃) with the [M(SC{O}R)₄][–] anion, no pure bimetallic compounds could be isolated. Hence, the synthetic route was slightly modified as follows. The bis-triphenylphosphine silver salts were premixed with the corresponding indium or gallium salts followed by the addition of the sodium thiocarboxylate. The reactions are summarized below (eq 2 or 3). These reactions yielded pure 3–5.



However, under similar conditions we were unable to isolate [(Ph₃P)₂AgGa(SC{O}Me)₄]. Attempts to syn-

Table 2. Selected Bond Lengths (Å) and Angles (deg) of 1

Bond Lengths			
Cu(1)–S(1)	2.488(2)	Cu(1)–S(2)	2.265(2)
Cu(1)–S(3)	2.266(2)	Cu(1)–P(1)	2.266(2)
Ga(1)–S(1)	2.268(2)	Ga(1)–S(4)	2.240(2)
Ga(1)–O(2)	1.870(5)	Ga(1)–O(3)	1.879(5)
S(1)–C(1)	1.788(8)	S(2)–C(2)	1.666(7)
S(3)–C(3)	1.671(8)	S(4)–C(4)	1.767(8)
O(1)–C(1)	1.222(9)	O(2)–C(2)	1.280(8)
O(3)–C(3)	1.256(8)	O(4)–C(4)	1.229(9)
Bond Angles			
S(2)–Cu(1)–S(1)	107.66(8)	S(3)–Cu(1)–S(1)	102.26(7)
S(2)–Cu(1)–S(3)	119.17(9)	P(1)–Cu(1)–S(1)	113.17(7)
S(2)–Cu(1)–P(1)	105.94(8)	S(3)–Cu(1)–P(1)	108.86(7)
S(4)–Ga(1)–S(1)	117.69(8)	O(2)–Ga(1)–S(1)	121.2(2)
O(3)–Ga(1)–S(1)	113.8(2)	O(2)–Ga(1)–S(4)	99.1(2)
O(3)–Ga(1)–S(4)	102.2(2)	O(2)–Ga(1)–O(3)	99.7(3)
Ga(1)–S(1)–Cu(1)	79.39(6)	C(1)–S(1)–Cu(1)	110.6(3)
C(2)–S(2)–Cu(1)	111.5(3)	C(3)–S(3)–Cu(1)	113.3(2)
C(1)–S(1)–Ga(1)	90.5(3)	C(4)–S(4)–Ga(1)	96.9(3)
C(2)–O(2)–Ga(1)	132.6(5)	C(3)–O(3)–Ga(1)	133.6(5)
O(1)–C(1)–S(1)	118.7(6)	O(2)–C(2)–S(2)	125.8(6)
O(3)–C(3)–S(3)	124.9(5)	O(4)–C(4)–S(4)	120.8(7)

thesize 4 and 5 at room temperature led to decomposition of the compounds, hence they were synthesized at 0 °C.

Structure of [(PPh₃)Cu(μ-SC{O}Ph-S)(μ-SC{O}Ph-S,O)₂Ga(SC{O}Ph)] (1). A perspective view of 1 is shown in Figure 1 and selected bond lengths and angles are given in Table 2. In 1, both the metal atoms, Cu(1) and Ga(1), are present in distorted tetrahedral geometry. The copper atom is bonded to one triphenylphosphine ligand and three sulfur atoms of three thiobenzoate ligands. All three thiobenzoate ligands bridge the two metal centers: two PhC{O}S[–] anions through a μ₂-S,O, and the other in a μ₂-S fashion. The distorted tetrahedral coordination environment at Ga(1) is made up by a S₂O₂ donor set. The P(1)–Cu(1)

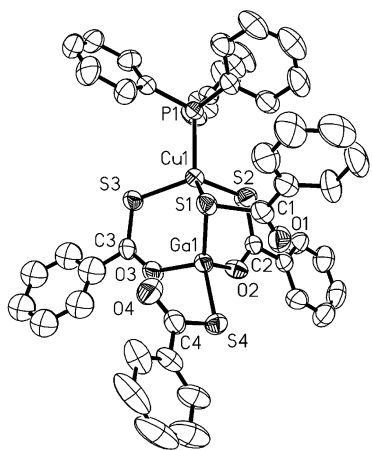


Figure 1. ORTEP diagram (with 50% probability of displacement ellipsoids) showing the molecular structure of **1**. Hydrogen atoms have been omitted for clarity.

distance, 2.266(2) Å) observed in **1** is normal.²² The Cu(1)–S(1) distance, 2.488(2) Å, is longer than Cu(1)–S(2) and Cu(1)–S(3) (2.265(2) and 2.266(2) Å, respectively) because S(1) is also involved in bonding to the Ga atom. The Cu–S distances from bridging sulfur atoms are expected to be longer than those from non-bridging ligands.^{21,22,24} Further, the shortening of C–S and lengthening of C–O distances may be attributed to the delocalization of electrons at the thiocarboxylate groups containing C(2) and C(3) atoms. A similar trend was observed in the other triphenylphosphinecopper thiocarboxylate compounds.²² The Ga(1)–S(1) and Ga(1)–S(4) distances, 2.268(2) and 2.240(2) Å, respectively, are not equal as expected for the bridging and terminal Ga–S bonds. The Ga(1)–O(2) and Ga(1)–O(3) distances, 1.870(5) and 1.879(5) Å respectively, fall within the range of established Ga–O distances (1.780–2.020 Å) obtained from the Cambridge Structure Database.³³ The Ga(1)–O(1) and Ga(1)–O(4) distances, 2.690(6) and 2.913(7) Å, respectively, are significantly less than the sum of van der Waals radii, 3.4 Å, and represent very weak interactions. Further, the distorted tetrahedral geometry at Ga(1) (99.1–121.2°) appears to support this.

Structure of [(PPh)₃Cu(μ-S-C(O)Ph-S,O)₂(μ₂-SC(O)Ph-S₂O)In(SC(O)Ph)] (2**).** A view of **2** is shown in Figure 2 and selected bond lengths and angles are given in Table 3. Compound **2** is a bimetallic compound containing copper and indium atoms. Of these, Cu(1) is bonded to one triphenylphosphine ligand and three thiobenzoate anions through their sulfur donor sites forming a tetrahedral PCuS₃ core as in **1**. Three thiobenzoate anions bridge the two metal ions through two μ₂-S,O and one μ₂-S₂O bonding modes. The fourth thiobenzoate anion chelates the indium metal atom. The coordination environment about the In(1) atom is thus distorted octahedral with a InO₄S₂ core. The P(1)–Cu(1) distance, 2.283(1) Å, is slightly longer than the corresponding bond distance observed in **1**. The Cu(1)–S(1) and Cu(1)–S(2) distances (2.265(1) and 2.281(1) Å, respectively) are longer than the Cu(1)–S(3) distance (2.470(1) Å) because of different types of bonding modes as explained above for **1**. It was also observed that the

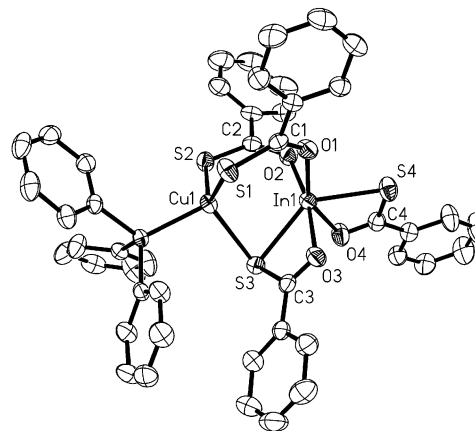


Figure 2. Thermal ellipsoid plot showing a view of **2**. Hydrogen atoms are not shown.

Table 3. Selected Bond Lengths (Å) and Angles (deg) of **2**

Bond Lengths			
Cu(1)–S(1)	2.265(1)	Cu(1)–S(2)	2.281(1)
Cu(1)–S(3)	2.470(1)	Cu(1)–P(1)	2.283(1)
In(1)–S(3)	2.537(1)	In(1)–S(4)	2.503(1)
In(1)–O(1)	2.126(3)	In(1)–O(2)	2.139(3)
In(1)–O(3)	2.372(3)	In(1)–O(4)	2.386(3)
In(1)–Cu(1)	3.068(1)	S(1)–C(1)	1.679(4)
S(2)–C(2)	1.680(4)	S(3)–C(3)	1.762(4)
S(4)–C(4)	1.726(4)	O(1)–C(1)	1.275(4)
O(2)–C(2)	1.273(4)	O(3)–C(3)	1.239(4)
O(4)–C(4)	1.240(4)	In(1)···Cu(1)	3.068(1)
Bond Angles			
S(1)–Cu(1)–S(2)	118.58(4)	S(1)–Cu(1)–S(3)	114.95(4)
S(2)–Cu(1)–S(3)	104.06(4)	S(1)–Cu(1)–P(1)	109.95(4)
S(2)–Cu(1)–P(1)	106.26(4)	P(1)–Cu(1)–S(3)	101.34(4)
S(4)–In(1)–S(3)	136.62(4)	O(1)–In(1)–S(3)	124.76(7)
O(2)–In(1)–S(3)	108.43(7)	O(3)–In(1)–S(3)	63.38(7)
O(4)–In(1)–S(3)	83.97(7)	O(1)–In(1)–S(4)	89.37(7)
O(2)–In(1)–S(4)	96.19(7)	O(3)–In(1)–S(4)	94.86(7)
O(4)–In(1)–S(4)	63.30(7)	O(1)–In(1)–O(2)	89.8(1)
O(1)–In(1)–O(3)	89.4(1)	O(2)–In(1)–O(3)	168.92(9)
O(1)–In(1)–O(4)	150.9(1)	O(2)–In(1)–O(4)	83.9(1)
O(3)–In(1)–O(4)	101.9(1)	C(1)–S(1)–Cu(1)	112.2(1)
C(2)–S(2)–Cu(1)	114.9(1)	C(3)–S(3)–Cu(1)	105.7(1)
Cu(1)–S(3)–In(1)	75.55(3)	C(3)–S(3)–In(1)	80.2(1)
C(4)–S(4)–In(1)	81.1(1)	C(1)–O(1)–In(1)	129.5(2)
C(2)–O(2)–In(1)	130.2(2)	C(3)–O(3)–In(1)	98.4(2)
C(4)–O(4)–In(1)	96.6(2)	O(1)–C(1)–S(1)	124.6(3)
O(2)–C(2)–S(2)	125.5(3)	O(3)–C(3)–S(3)	117.7(3)
O(4)–C(4)–S(4)	119.0(3)		

In(1)–O(1) and In(1)–O(2) distances (2.126(3) and 2.139(3) Å, respectively) are shorter than the In(1)–O(3) and In(1)–O(4) distances (2.372(3) and 2.386(3) Å, respectively). The former In–O distances fall in the upper range of distances observed in a few indium alkoxide compounds, 1.969–2.152 Å.³⁴ The shorter In–O distance may be attributed to extra negative charges acquired by O(1) and O(2) due to the delocalization of electrons in these thiocarboxylate groups. The lengthening of C–O and shortening of C–S bonds appear to suggest this. On the other hand, the longer In–O distances may be attributed to the weakening of the bond between In(III) and neutral carbonyl oxygen atom as indicated by the C=O distances in Table 3. The thiobenzoate ligands adopt three types of bonding modes: a terminal chelating mode, a bridging mode with the O atoms linked to indium and the S atoms to copper, and a terminal chelating mode with an additional Cu–S bond. The nonbonding distance Cu(1)···

(33) Allen, F. H.; Davies, J. E.; Galloy, J. J.; Johnson, O.; Kennard, O.; Macreac, C. F.; Mitchell, E. M.; Mitchell, G. F.; Smith, J. M.; Watson, D. G. *J. Chem. Inf. Comput. Sci.* **1991**, *31*, 187.

(34) Suh, S.; Hoffman, D. M. *J. Am. Chem. Soc.* **2000**, *122*, 9396.

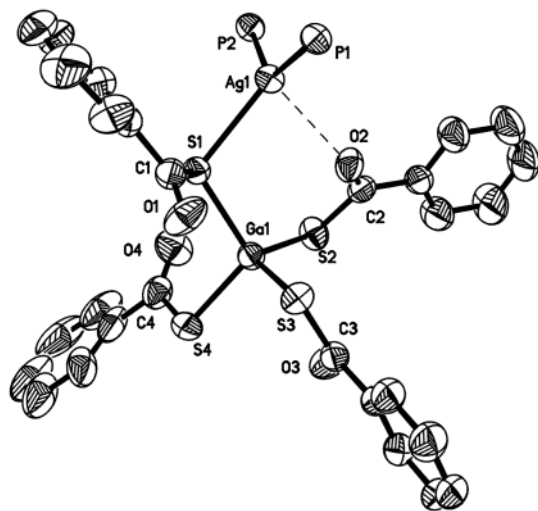


Figure 3. Perspective view of **3**.

Table 4. Selected Bond Lengths (Å) and Angles (deg) of **3**

Bond Lengths			
Ag(1)–S(1)	2.623(2)	Ag(1)–P(1)	2.451(2)
Ag(1)–P(2)	2.455(2)	Ga(1)–S(1)	2.309(2)
Ga(1)–S(2)	2.271(2)	Ga(1)–S(3)	2.273(2)
Ga(1)–S(4)	2.271(2)	S(1)–C(1)	1.778(6)
S(2)–C(2)	1.761(6)	S(3)–C(3)	1.766(6)
S(4)–C(4)	1.761(7)	O(1)–C(1)	1.193(7)
O(2)–C(2)	1.216(7)	O(3)–C(3)	1.198(7)
O(4)–C(4)	1.215(8)		
Bond Angles			
P(1)–Ag(1)–S(1)	120.86(5)	P(2)–Ag(1)–S(1)	105.66(5)
P(1)–Ag(1)–P(2)	129.14(5)	S(2)–Ga(1)–S(1)	106.21(6)
S(3)–Ga(1)–S(1)	115.00(6)	S(4)–Ga(1)–S(1)	107.10(6)
S(2)–Ga(1)–S(3)	112.99(6)	S(2)–Ga(1)–S(4)	113.00(7)
S(4)–Ga(1)–S(3)	102.55(7)	Ga(1)–S(1)–Ag(1)	109.26(6)
C(1)–S(1)–Ag(1)	99.5(2)	C(1)–S(1)–Ga(1)	104.4(2)
C(2)–S(2)–Ga(1)	97.5(2)	C(3)–S(3)–Ga(1)	97.4(2)
C(4)–S(4)–Ga(1)	101.1(3)	O(1)–C(1)–S(1)	121.6(5)
O(2)–C(2)–S(2)	122.9(5)	O(3)–C(3)–S(3)	123.2(5)
O(4)–C(4)–S(4)	121.9(5)		

In(1), 3.068(1) Å, is shorter than the sum of their van der Waals radii (3.3 Å)³⁵ as was also observed in (Ph₃P)₂-Cu(*μ*-SEt)₂In(SEt)₂, (Ph₃P)₂Cu(*μ*-SeEt)₂In(SEt)₂, and (Ph₃P)₂Cu(*μ*-S(*iso*-Bu))₂In(S(*iso*-Bu))₂, which are 3.34, 3.32, and 3.24 Å, respectively.¹⁰ The origin of this bond shortening has not been investigated further. However, the longer Cu–P distance, 2.283(1) Å, as compared to **1** may be a consequence of this Cu··In weak interaction. The In(1) has a highly distorted octahedral environment with S₂O₄ donor set. The In–S distances, 2.537(1) and 2.503(1) Å, are comparable to 2.457(1)–2.542(1) Å observed in **5** which also has highly distorted octahedral geometry at In(III).²⁸

Structure of [(Ph₃P)₂Ag(*μ*-SC{O}Ph-S)Ga(SC{O}Ph)₃] (3**).** A perspective view of **3** is shown in Figure 3 and selected bond lengths and angles are listed in Table 4. Compound **3** crystallizes with 3.5 CHCl₃ molecules. It consists of one anionic [Ga(SC{O}Ph)₄] and a cationic [(Ph₃P)₂Ag] unit. All four thiobenzoate anions are S-bonded to the gallium ion, Ga(1), and hence it has a tetrahedral GaS₄ core. One thiobenzoate anion adopts a sulfur atom, S(1) in its bridging mode to bind Ga(1) and Ag(1). The distance between Ag(1) and O(2), 2.626(3) Å, is far less than the sum of the van der Waals radii (3.2 Å) suggesting that there may be weak interaction

Table 5. Pyrolysis and TGA Results for **1–5**

compd	TG results			product of decomposition
	temp range (°C)	residual wt obsd (calcd) (%)	residual wt from pyrolysis ^a (%)	
1	150–327	25.5 (20.9)	20.8	CuGaS ₂ ^b
2	168–350	24.3 (24.5)	24.0	CuInS ₂ ^c
3	185–349	18.9 (19.3)	19.3	AgGaS ₂ ^d
4	132–315	28.4 (27.4)	27.9	AgInS ₂ ^e
5	175–328	23.6 (22.1)	22.1	AgInS ₂ ^e

^a The samples were heated at 300 °C under a 0.5 Torr pressure for 30 min. ^b Tetragonal CuGaS₂ (JCPDS Code 06-0358). ^c Tetragonal CuInS₂ (JCPDS Code 27-0159); ^d Tetragonal AgGaS₂ (JCPDS 27-0615). ^e Orthorhombic AgInS₂ (JCPDS Code 25-1328).

between these two atoms in the solid state. However, the sum of the bond angles, 355.66° supports trigonal planar geometry at Ag(1) and a slight deformation of the geometry due to Ag··O close contact. The Ga–S distances in **3** fall in the range 2.271(2)–2.309(2) Å which are comparable to the Ga–S distances observed in [Et₃NH][Ga(SC{O}Ph)₄].³⁶ The Ag(1)–P(1) and Ag(1)–P(2) distances, 2.451(2) and 2.455(2) Å, respectively, are comparable to those observed in **5**.²⁸ A weak interaction appears to exist between Ga(1) and O(2) (2.626(4) Å) which is significantly lower than the sum of the van der Waals radii of 3.4 Å.

The structures of **1** and **2** exhibit subtle differences in the bonding modes of the thiocarboxylate anion. In **1**, *μ*₂-S,O and *μ*₂-S bonding modes are displayed, whereas in **2**, *μ*₂-S,O and *μ*₂-S₂,O are observed. These changes in bonding modes may be attributed to the change in the size of the metal atoms. The bimetallic compounds of Ag and Ga/In show interesting structural features. In **3**, the metal atoms Ag and Ga are bridged by a thiobenzoate anion through a *μ*₂-S bonding while another thiobenzoate ligand bonded to the gallium metal atom weakly interacts with the silver metal atom through its oxygen donor site. On the other hand, the Ag and In metal centers are bridged by two PhC{O}S⁻ ligands in **5**.²⁸ Furthermore, the Cu–Ga and Cu–In distances in **1** and **2**, respectively, are shorter than the sums of their van der Waals radii, while the Ag–In distance in **5** is not. The soft Cu atom is always bonded to the soft S donor sites; the harder Ga atoms accept S and O donor centers but its site does allow a coordination number of four in these compounds. The larger In atom achieves a coordination number of six by bonding the thiocarboxylate ions in a chelating mode.

Thermogravimetric and Pyrolysis Studies. The usefulness of **1–5** as single-source precursors for ternary sulfide materials was investigated by thermogravimetry and pyrolysis experiments. The TG curves are presented in Figure 4 and the results are tabulated in Table 5. The loss of dichloromethane in **2** was observed in the temperature range 79–111 °C. The observed weight loss, 6.3%, matched well with the calculated value, 6.4%, for the loss of a half molecule of CH₂Cl₂. It is unusual that CH₂Cl₂ is lost at such a high temperature. The elemental analysis of **2** also indicated the presence of half a CH₂Cl₂ molecule per formula unit. This suggests that the CH₂Cl₂ molecules are strongly occluded in **2**. The TG experiment on solvent-free **2** confirmed that the initial weight loss is indeed due to the loss of CH₂Cl₂.

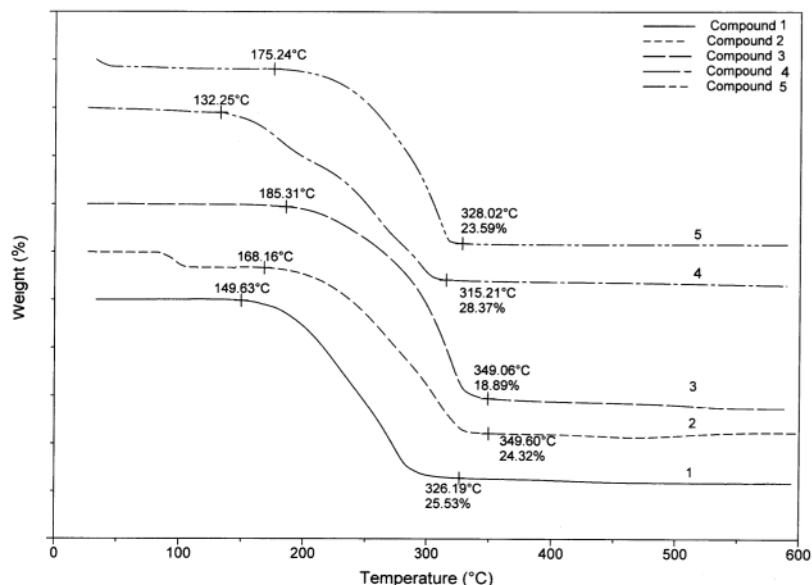
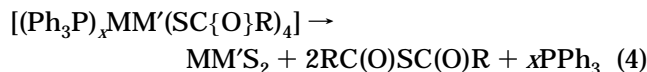


Figure 4. Thermogravimetric curves of 1–5.

TG data reveal that the compounds decompose in the temperature range 150–350 °C in unresolved multiple steps to stable final products, which were found to be the corresponding ternary sulfides. The residual masses for 1–5 agree with the formation of the ternary sulfides except for 1 as shown in Table 4. The residue of 1 probably contains some side products of decomposition. On the basis of the thermal decomposition pathway of metal thiocarboxylates discussed by Hampden-Smith^{37–41} the decomposition reaction may be described as in eq 4.



To identify the nature of the ternary materials obtained, all compounds were subjected to pyrolysis at 300 °C at a pressure of 0.5 Torr for 30 min. The ternary materials thus obtained were characterized by X-ray powder diffraction, EDAX, and SEM. The XRPD patterns are shown in Figure 5. The residues obtained from 1 and 2 matched the tetragonal phases of CuGaS₂ and CuInS₂ (JCPDS database). Pyrolysis of 3 resulted in formation of tetragonal AgGaS₂. The X-ray powder diffraction patterns of these residues suggested a high degree of crystallinity. The EDAX profiles of the samples show peaks for all the corresponding elements, as well as peaks for carbon, due to incorporated graphite mesh and oxygen due to aerobic conditions. The copper/gallium/sulfur and copper/indium/sulfur ratios were found to be 1:1.12:1.82 and 1:1.08:1.89, respectively, confirming the stoichiometry of these compounds. The SEM images (Supporting Information) of the ternary materials showed a wide distribution of particle sizes

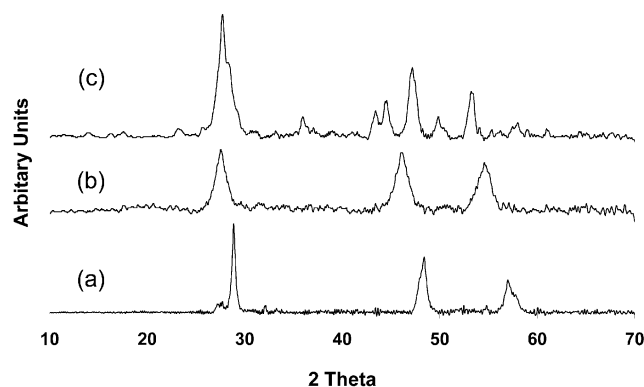


Figure 5. X-ray powder diffraction patterns of (a) CuGaS₂ from 1, (b) CuInS₂ from 2, and (c) AgGaS₂ from 3 by pyrolysis.

for the sulfide materials which account for the broad peaks observed in their X-ray powder diffraction patterns. The particle size of the sulfide materials ranges from 5 to 50 μm.

Aerosol-Assisted Chemical Vapor Deposition of [(Ph₃P)_xCu(SC{O}Ph)₃In(SC{O}Ph)]. Attempts to deposit thin films using 2 as a single-source precursor by aerosol-assisted chemical vapor deposition resulted in predominantly β-In₂S₃ materials rather than the expected CuInS₂, as was observed from TGA and pyrolysis studies. In most cases, dark yellow β-In₂S₃ films were obtained at growth temperatures of 350–450 °C after 2 h of growth confirmed by XRPD. There were no differences on using different solvents such as THF or toluene. Figure 6 indicates the XRPD pattern of β-In₂S₃ film grown on glass from 2 in toluene at 450 °C after 2 h growth. Broad peaks indicate that crystallinity of the particles is relatively poor and a preferred orientation along the (311) plane is found. Nomura et al. reported the growth of CuIn₅S₈ films from BuIn(SⁿPr)Cu(S₂CNⁿPr₂) by LP-MOCVD.⁴² In their study, a higher growth temperature (450 °C) resulted in films of β-In₂S₃, whereas at lower growth temperatures the films consisted of CuIn₅S₈.

XPS was employed to determine photoelectron binding energies of the elements comprising the films grown

(37) Shang, G.; Hampden-Smith, M. J.; Duesler, E. N. *Chem. Commun.* **1996**, 1733.

(38) Shang, G.; Kunze, K.; Hampden-Smith, M. J.; Duesler, E. N. *Chem. Vap. Deposition* **1996**, *2*, 242.

(39) Nyman, M. D.; Hampden-Smith, M. J.; Duesler, E. N. *Chem. Vap. Deposition* **1996**, *2*, 171.

(40) Nyman, M. D.; Jenkins, K.; Hampden-Smith, M. J.; Kostas, T. T.; Duesler, E. N.; Rheingold, A. L.; Liable-Sands, M. L. *Chem. Mater.* **1998**, *10*, 914.

(41) Nyman, M. D.; Hampden-Smith, M. J.; Duesler, E. N. *Inorg. Chem.* **1997**, *36*, 2218.

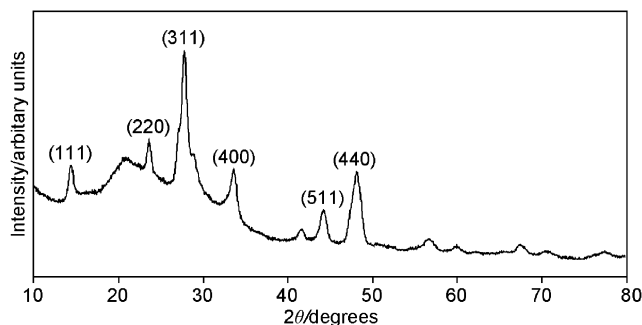


Figure 6. XRPD pattern of a β - In_2S_3 film grown from a solution of compound **2** in toluene at 450 °C by AACVD.

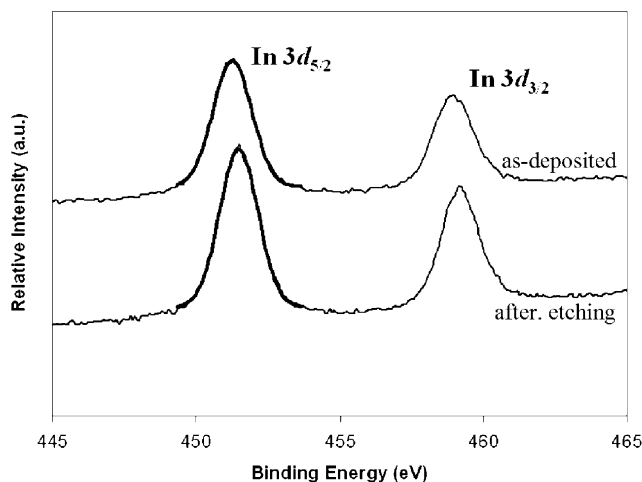


Figure 7. XPS spectra of In 3d peaks of a β - In_2S_3 film as-deposited and after 1 h of etching.

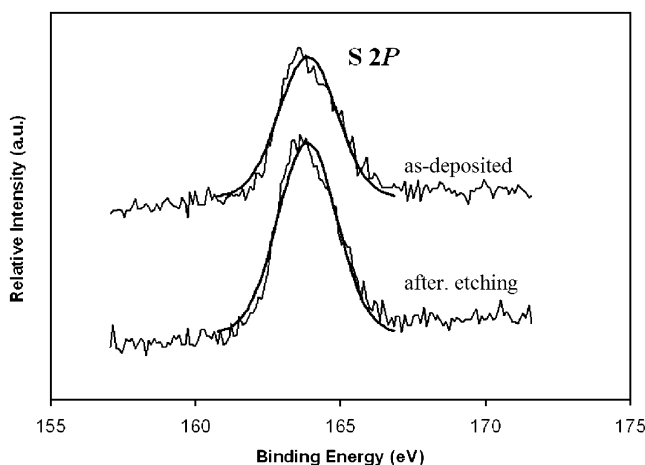
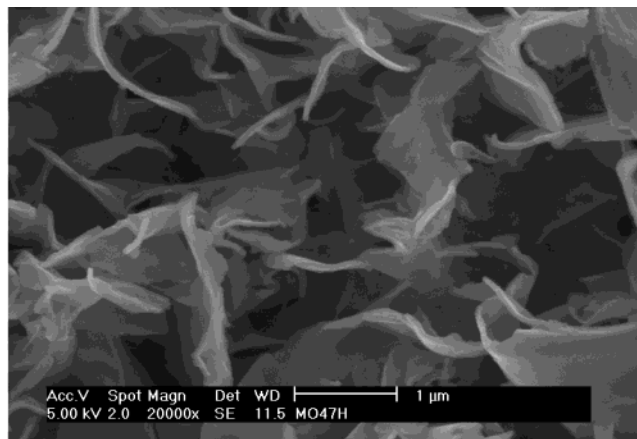


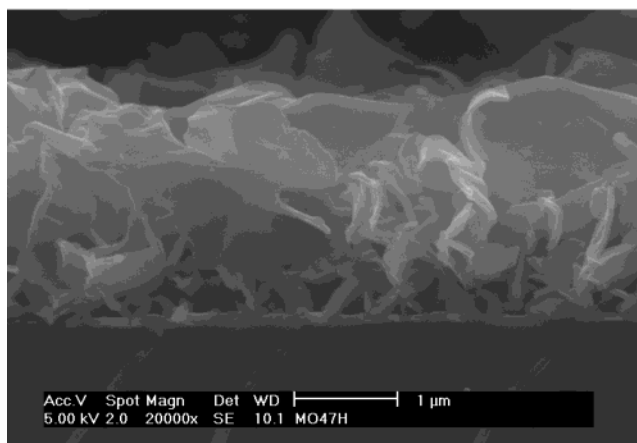
Figure 8. XPS spectra of S 2s peaks of a β - In_2S_3 film as-deposited and after 1 h of etching.

from **2** in toluene at 450 °C after 2 h growth. Figures 7 and 8 show In 3d and S 2p peaks observed before etching and after 1 h of etching. The peaks obtained before and after etching are not significantly different in terms of their binding energies and intensities. Indium 3d peaks were found at 451.5 eV (In 3d_{5/2}) and 458.6 eV (In 3d_{3/2}) before etching and 451.3 eV (In 3d_{5/2}) and 458.2 eV (In 3d_{3/2}) after etching. Sulfur 2p peaks were found at 163.9 eV in both cases. Relative atomic

(42) Nomura, R.; Seki, Y.; Matsuda, H. *Thin Solid Films* **1992**, *209*, 145.



(a)



(b)

Figure 9. SEM images of a In_2S_3 film grown from the solution of toluene and compound **2** at 450 °C: (a) top view, (b) cross-section view.

percentages of indium and sulfur were found to be slightly variable depending on etching treatment (2:3.66 before etching and 2:3.29 after etching).

SEM studies on the In_2S_3 films show that the particles are randomly oriented on the glass substrate (Figure 9) with ca. 1.5 $\mu\text{m}/\text{h}$ growth rate. There was also no evidence for copper peaks in the EDAX spectra but in some cases small traces of copper were observed (ca. <1%). This observation suggests that there was a pre-reaction between the precursor and the solvents used in this study during the CVD process. ESI-MS of **2** showed no molecular ion peak, however, signals due to $[\text{In}(\text{SC}\{\text{O}\}\text{Ph})_4]^-$, $[(\text{PPh}_3)_2\text{Cu}]^+$, and $[(\text{PPh}_3)_3\text{Cu}]^+$ were present. This indicates the dissociation of the compound in the solution. Such processes are common among phosphine adducts of coinage metal salts and have been substantiated by various techniques including NMR, molecular weight determinations, and conductivity measurements.^{43–46} Our finding of dissociation, using

(43) Muetterties, E. L.; Alegranti, C. W. *J. Am. Chem. Soc.* **1972**, *94*, 6386.

(44) Barron, P. F.; Dyason, J. C.; Healy, P. C.; Engelhardt, L. M.; Skelton, B. W.; White, A. H. *J. Chem. Soc., Dalton Trans.* **1986**, 1965.

(45) Nakajima, H.; Matsumoto, K.; Tanaka, K.; Tanaka, T. *Inorg. Nucl. Chem.* **1975**, *37*, 2463.

(46) Black, J. R.; Levason, W.; Spicer, M. D.; Webster, M. *J. Chem. Soc., Dalton Trans.* **1993**, 3129.

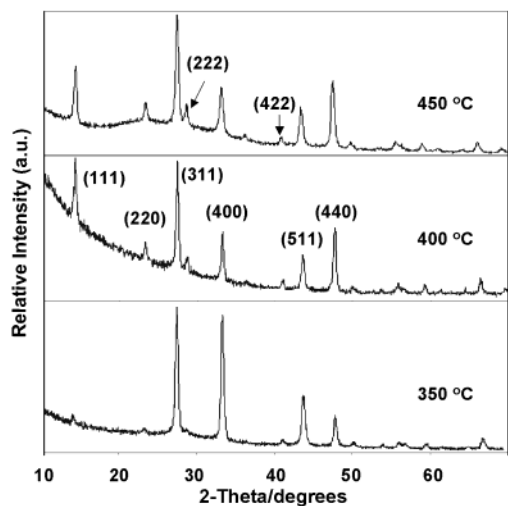


Figure 10. X-ray powder diffraction pattern of AgIn_5S_8 thin films formed from **4**.

ESIMS, also concurs with the findings of Henderson et al.⁴⁷

Aerosol-Assisted Chemical Vapor Deposition of $[(\text{Ph}_3\text{P})_2\text{Ag}(\text{SC}(\text{O})\text{R})_3\text{In}(\text{SC}(\text{O})\text{R})]$ ($\text{R} = \text{Me}$ (4**); Ph (**5**)).** Aerosol-assisted chemical vapor deposition (AACVD) of THF solution of **4** and **5** yielded AgIn_5S_8 films. Films grown on glass at 350, 400, and 450 °C from **4** were transparent and adherent (Scotch tape test) with a dark red color, and films grown at 350 °C were slightly red. XRPD analysis (step size 0.04°/2 s) confirmed that the films prepared from compounds **4** and **5** were found to be cubic- AgIn_5S_8 (JCPDS 25-1329) with a preferred

orientation along the (311) plane (Figure 10). XRPD patterns of films grown from **4** showed the (111) and (222) planes were noticeably enhanced with increasing growth temperature, and intensities of peaks from the (511) and (440) planes were also reversed. XRPD measurements of films from compound **5** indicate similar patterns but no indication of enhancement of peak intensities was observed in the case of the films grown from **4**.

Scanning electron microscopy (SEM) images (Figure 11) of the AgIn_5S_8 films obtained from **4** show the dramatic changes in the morphology of films grown as a function of growth temperatures. The morphology of the films grown on glass at 450 °C (Figure 11c) consists of thin platelike particles, positioned laid down onto the substrate with random orientation, and a similar morphology was also found in the films grown on Si(100) substrates at the same temperature. However, with decreasing the growth temperature to 400 or 350 °C, the morphology becomes more dense and no platelike particles were formed (Figure 11a and b). Growth rate and average particle size of the films grown at 400 °C were ca. 0.3 $\mu\text{m}/\text{h}$ and ca. 0.5 μm , respectively, and at 350 °C were ca. 0.2 $\mu\text{m}/\text{h}$ and ca. 0.3 μm .

Morphologies of films grown from compound **5** (Figure 12) are quite different from those grown from **4**. Films obtained at a growth temperature of 350 °C revealed a relatively dense morphology and a smaller particle size (ca. 100–300 nm) than those prepared from higher growth temperatures. Particles on glass substrates (Figure 12c) grown at 450 °C have trigonal habits consisting of several layers. However, on changing the substrate from glass to Si(100), the formation of par-

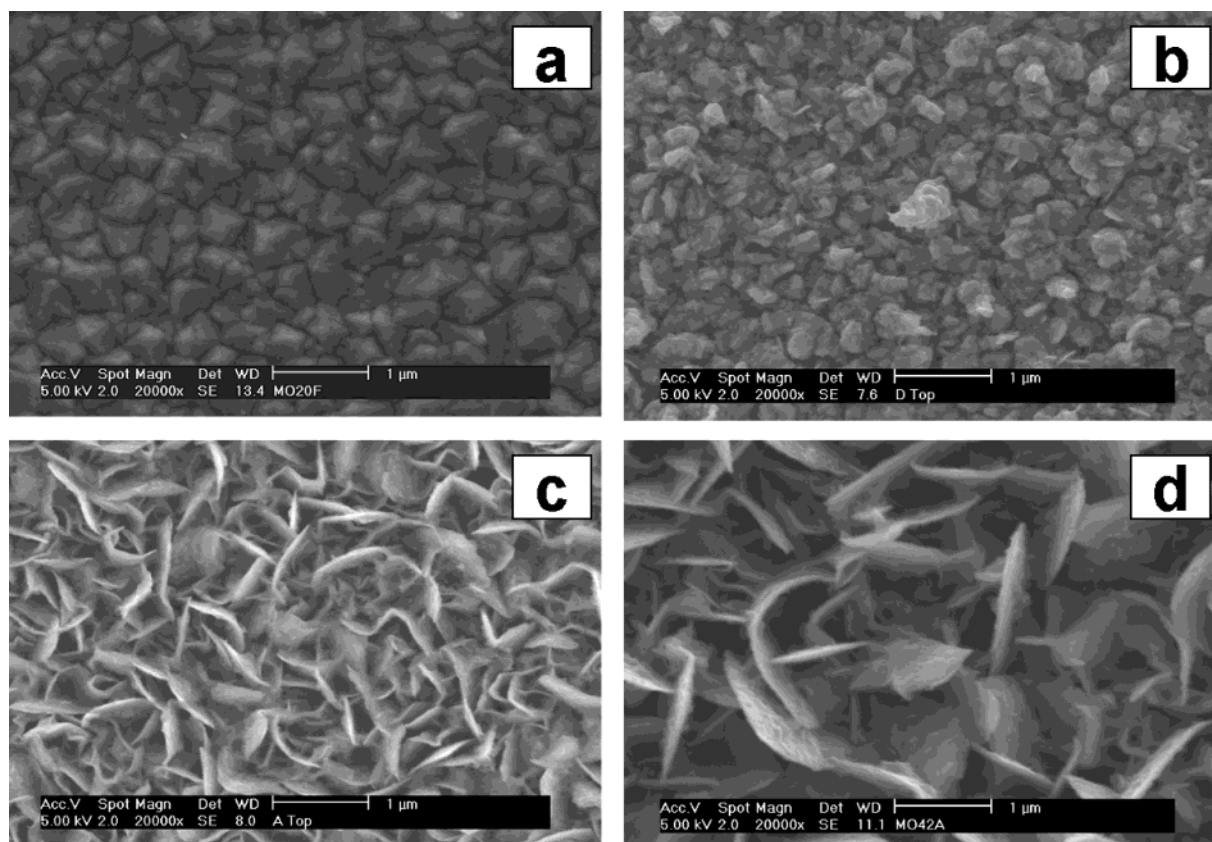


Figure 11. SEM images of AgIn_5S_8 films on glass grown from **4**: (a) 350 °C on glass, (b) 400 °C on glass, (c) 450 °C on glass, and (d) 450 °C on Si(100).

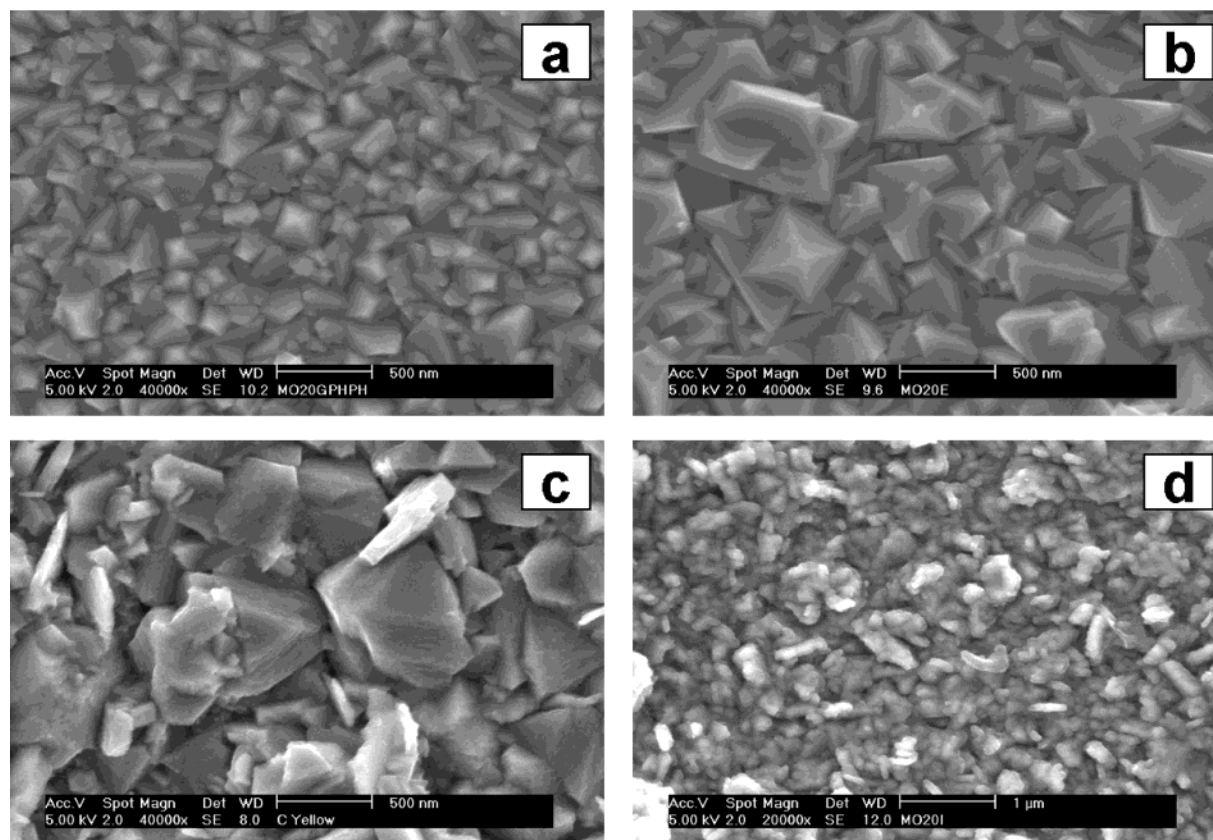


Figure 12. SEM images of AgIn₅S₈ films on glass grown from 5: (a) 350 °C on glass, (b) 400 °C on glass, (c) 450 °C on glass, and (d) 450 °C on Si(100).

ticles leads to rice-like instead of triangular shapes (Figure 12d). Growth rates obtained from cross-section views for the films were found to be ca. 0.2 $\mu\text{m/h}$ at 350 °C, 0.5 $\mu\text{m/h}$ at 400 °C, and 0.6 $\mu\text{m/h}$ at 450 °C on glass substrates after 2 h of growth.

Conclusion

In this paper, we have reported the syntheses and characterization of the compounds [(Ph₃P)CuM(SC(O)Ph)₄] (M = Ga (**1**) or In (**2**)) and [(Ph₃P)₂AgGa(SC(O)Ph)₄] (**3**). The structures of the three compounds have been determined by X-ray crystallography. Thermogravimetric analyses and pyrolysis studies of **1–5** indicate that these compounds decompose to give ternary MM'S₂ materials. Compounds **4** and **5** can also be

used as precursors for AgIn₅S₈ films as was demonstrated by AACVD experiments. These compounds may also have the potential to be used to prepare nanocrystalline sulfides via the single-source molecular precursor route.

Acknowledgment. We thank the National University of Singapore for a grant to J.J.V. (RP-143-000-084-112) and a graduate scholarship to T.C.D. P.O.B. thanks EPSRC, UK for support. J.J.V. thanks the Royal Society of Chemistry for the travel grant to visit Manchester, UK.

Supporting Information Available: SEM micrographs of the pyrolysis products of compounds **1–5** (PDF). This material is available free of charge via the Internet at <http://pubs.acs.org>.

(47) Bonnington, L. S.; Toll, R. K.; Gray, E. J.; Flett, J. I.; Henderson, W. *Inorg. Chim. Acta* **1999**, *290*, 213.